AOMSUC-15 2025 FYSUC

THE 15TH ASIA-OCEANIA METEOROLOGICAL SATELLITE USERS' CONFERENCE (AOMSUC-15)
2025 FENGYUN SATELLITE USER CONFERENCE (2025 FYSUC)

Passive Microwave Remote Sensing of Vegetation Properties

Jiancheng Shi, Oct. 29, 2025, Qindao, China

National Space Science Center, Chinese Academy of Sciences

Vegetation Properties Obtained from Satellites

Current most commonly used tools from optical sensors

NDIV – a measure of vegetation greenness from visible and near infrared spectrum;

LAI – a measure of total surface area of all leaves contained in a canopy over an unit area – a geometric parameter;

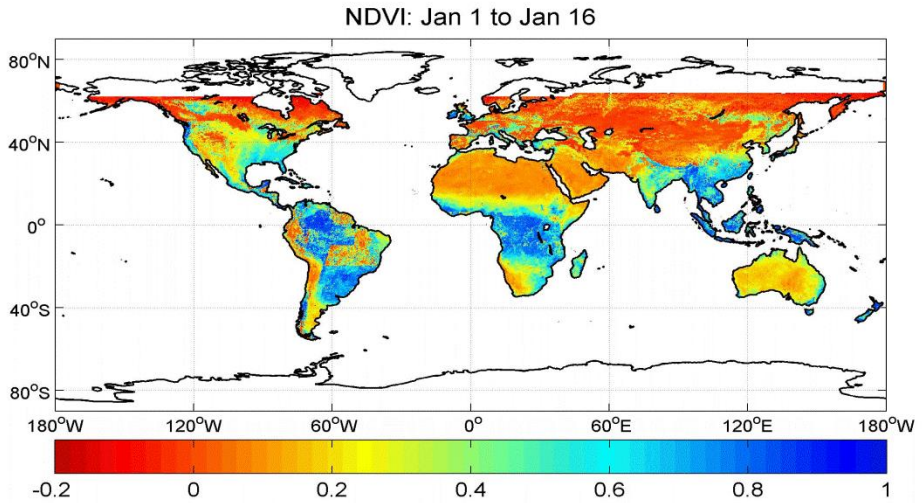

Advantage of Microwave sensors: Depending on frequency, not only sensitive to leafy part but also sensitive to woody part of vegetation information.

Facing problems:

- Atmospheric effects – optical sensors > microwave sensors;
- Background effects - microwave sensors > optical sensors;

Outline

- Deriving Microwave Vegetation Index (MVI) with Multi-frequency AMSR-E Data

- Deriving Microwave Vegetation Index (MVI) with Multi-angular SMOS Data
  - Methodology for retrieving vegetation optical depth and soil moisture

AMSR-E on AQUA Satellite

AMSR-E: Advanced Microwave Scanning Radiometer

Sensor Specifications

Frequency (GHz)	Polarization	Sensitivity (K)	Mean Spatial Resolution (km)	Swath (km)
6.925	V, H	0.3	56	1445
10.65	V, H	0.6	38	1445
18.7	V, H	0.6	21	1445
23.8	V, H	0.6	24	1445
36.5	V, H	0.6	12	1445
89.0	V, H	1.1	5.4	1445

- 12 channel, 6 frequency conically scanning passive microwave radiometer
- Earth incidence angle of 55°
- Built by the Japan Aerospace Exploration Agency (JAXA)

AQUA Satellite

- Launched on May 4, 2002
- Sun-synchronous orbit
- Equatorial crossing at 13:30 LST (ascending)

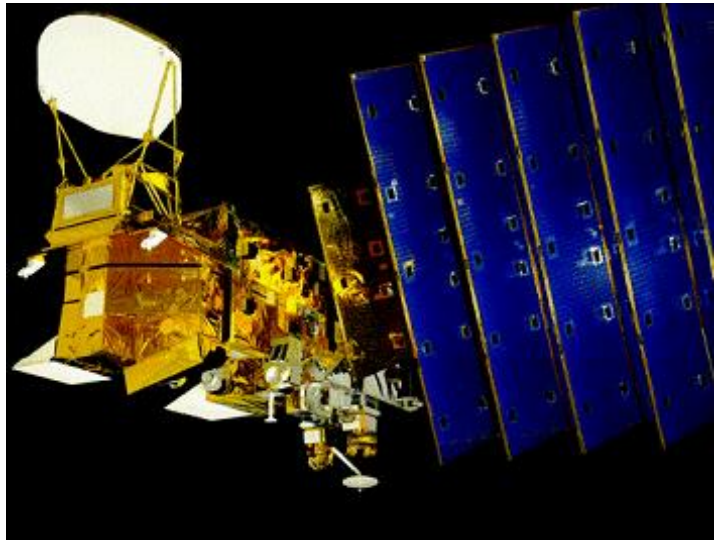

Microwave RT Model (ω-τ model)

At pixel scale, fraction of vegetation cover need to be considered

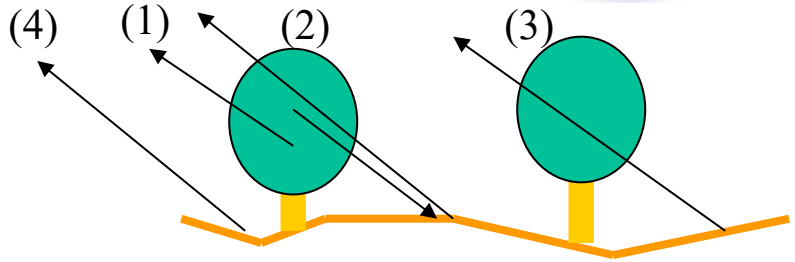

Four component emission model

$$E_p^t = f_v \cdot E_p^v + f_v \cdot E_p^v \cdot L_p \cdot R_p^e + f_v \cdot L_p \cdot E_p^s + (1 - f_v) \cdot E_p^s$$

For Tb

Re-range

$$T_{Bp}^t = f_v \cdot E_p^v (1 + L_p) \cdot Tv + E_p^s \cdot (1 - f_v + f_v \cdot L_p \cdot (1 - E_p^v)) \cdot Ts$$

Ve Vatt

$$T_{Bp}^t = V_e + E_p^s \cdot V_{att}$$

Subscript p: polarization; *Lp*: one-way attenuation factor;Superscripts *t, v*, and *s* are for total, vegetation, and surface terms;

Tv and Ts is temperatures for vegetation and ground surface;*fv* is vegetation fraction cover

Characteristics of Surface Components at Different Frequency

AIEM simulations with wide range soil moisture & roughness

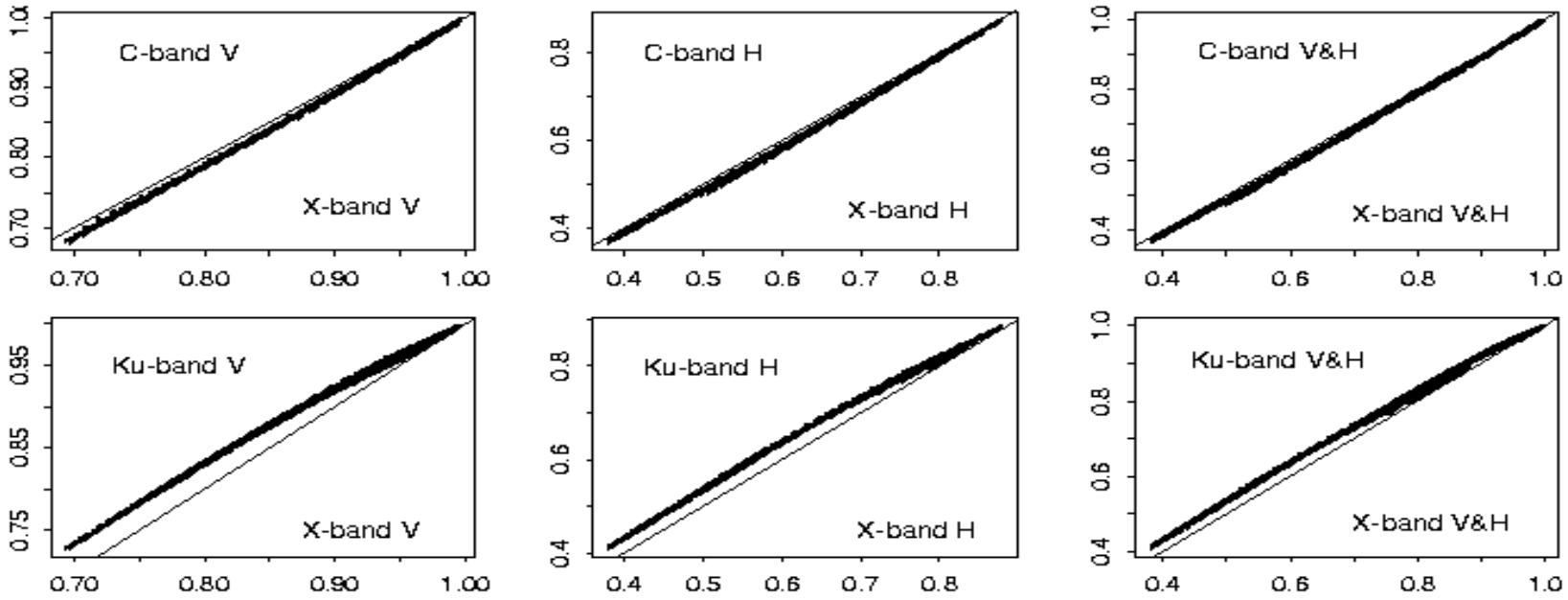

Surface component summary:

- Surface emissivity increases as frequency increases due to frequency dependence of water part of dielectric properties;
- Surface emissivities at two adjacent AMSR-E frequencies can be well correlated for all soil moisture and surface roughness conditions;
- They can be described as a linear function with the parameters are polarization independent.

Validation and Description of Surface Emission Relationship at Different Frequency

Experimental Data (BARC 1978-1982)

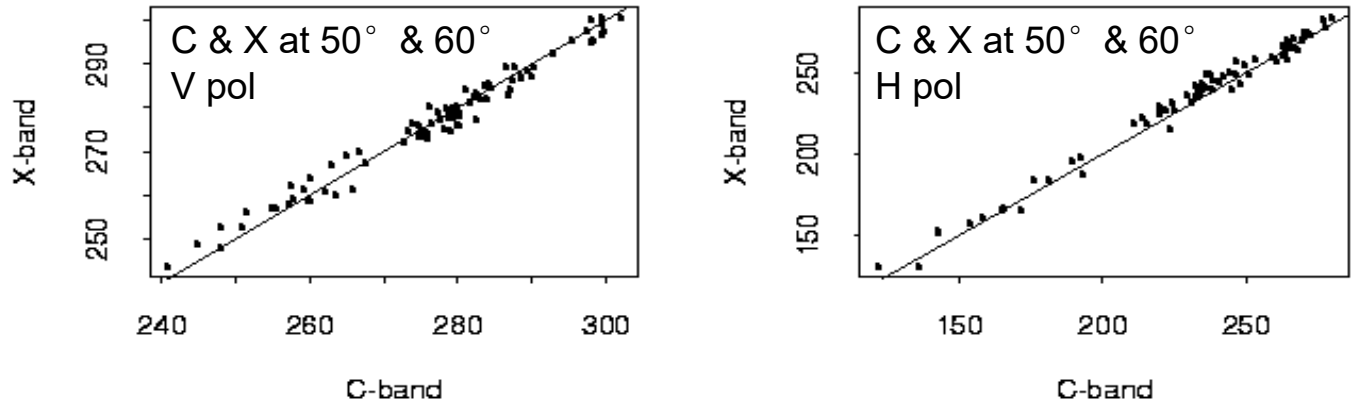

Linear function for surface emissivity at two adjacent AMSR-E frequencies:

$$Ep(f1) \approx a(f1,f2)+b(f1,f2)*Ep(f2)$$

Relative error in % of above equation from AIEM simulated data

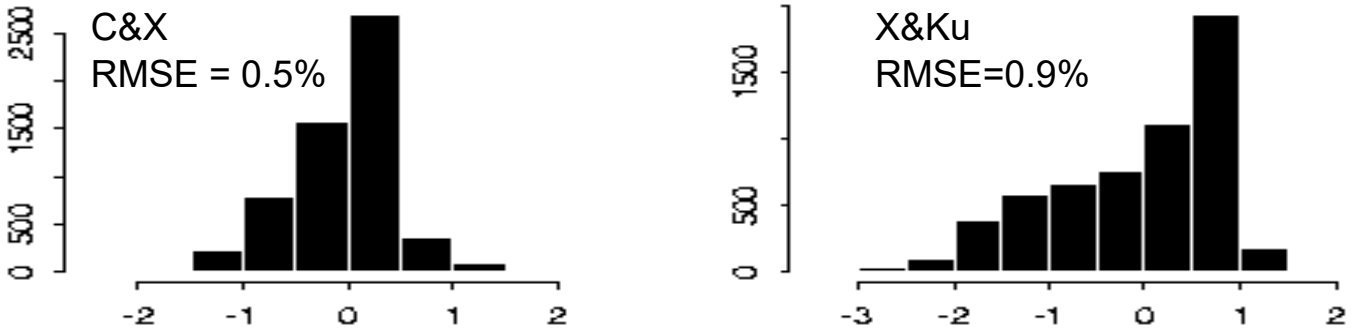

Relationship of TBs at Two Frequencies

$$T_{Bp}^{t} = V_e + E_p^s \cdot V_{att}$$

With two frequencies surface emission relation

$$E_p^s(f_1) = a(f_1, f_2) + b(f_1, f_2) \cdot E_p^s(f_2)$$

$$\frac{T_{Bp}^{t}(f_1) - V_e(f_1)}{V_{att}(f_1)} = a(f_1, f_2) + b(f_1, f_2) \cdot \frac{T_{Bp}^{t}(f_2) - V_e(f_2)}{V_{att}(f_2)}$$

$$T_{Bp}^{t}(f_1) = a(f_1, f_2) \cdot V_{att}(f_1) + V_e(f_1) - b(f_1, f_2) \cdot \frac{V_{att}(f_1)}{V_{att}(f_2)} \cdot V_e(f_2) + b(f_1, f_2) \cdot \frac{V_{att}(f_1)}{V_{att}(f_2)} \cdot T_{Bp}^{t}(f_2)$$

A_p B_p

Relationship of Tbs at two adjacent frequencies can be described as a linear function with its slope and intercept depending only on the vegetation properties.

A and B are defined as the Microwave Vegetation Indices – MVIs. They are independent of ground emission signals.

Microwave Vegetation Indices from Satellite

Assumption: no polarization dependence in vegetation components V_e and V_{att}

Directly solve two vegetation related components (slope and intercept) in the linear equations by the measurements

$$B(f_1, f_2) = \frac{T_{Bv}^t(f_1) - T_{Bh}^t(f_1)}{T_{Bv}^t(f_2) - T_{Bh}^t(f_2)}$$

$$A(f_1, f_2) = \frac{1}{2}\left(T_{Bv}^t(f_1) + T_{Bh}^t(f_1)\right) - \frac{1}{2} B(f_1, f_2) \cdot \left(T_{Bv}^t(f_2) + T_B^t(f_2)\right)$$

There are four Microwave Vegetation Indices that can be derived by AMSR-E measurements with a low frequency pair: A(C,X) and B(C,X), and with a high frequency pair: A(X,Ku) and B(X,Ku).

Data Processing

Strong RFI or snow effects

A < 0 and/or B > 1

Weak RFI and Atmospheric condition effects (rain and clouds)

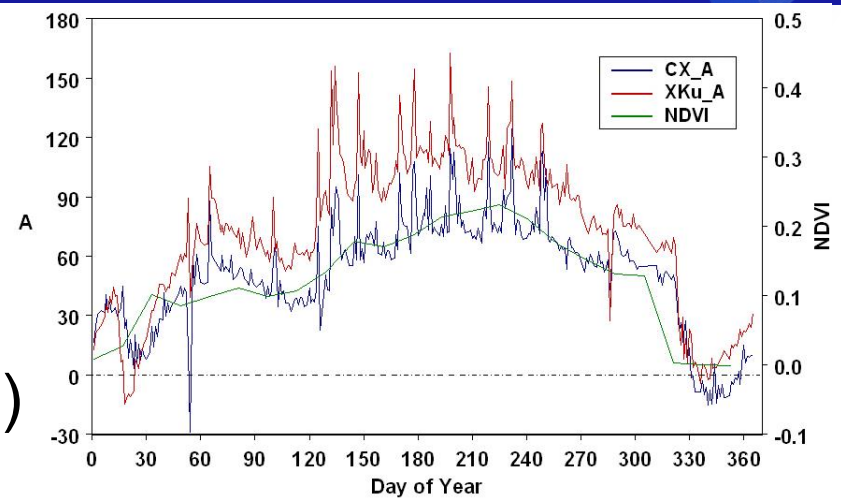

Median Filter

A and B Fluctuations

Data processing:

1. **Remove A < 0 or B > 1**
2. **Run a median filter**

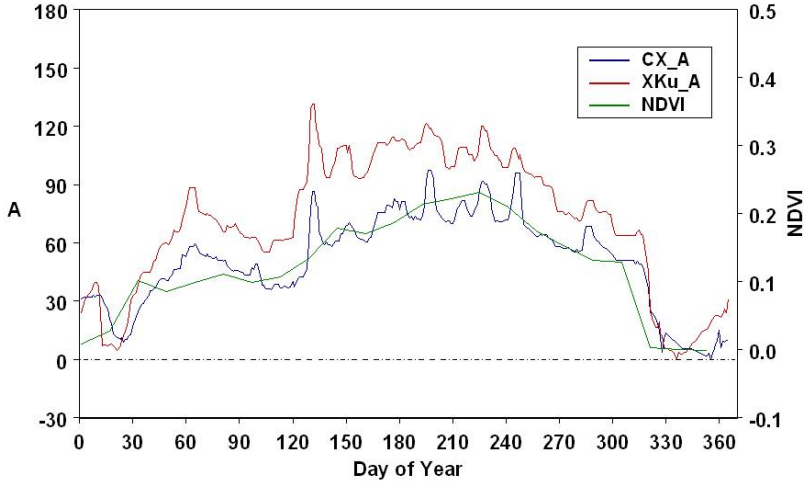

Comparison of Monthly Mean MVIs (AMSR-E) with NDVI & LAI (MODIS) in April and July

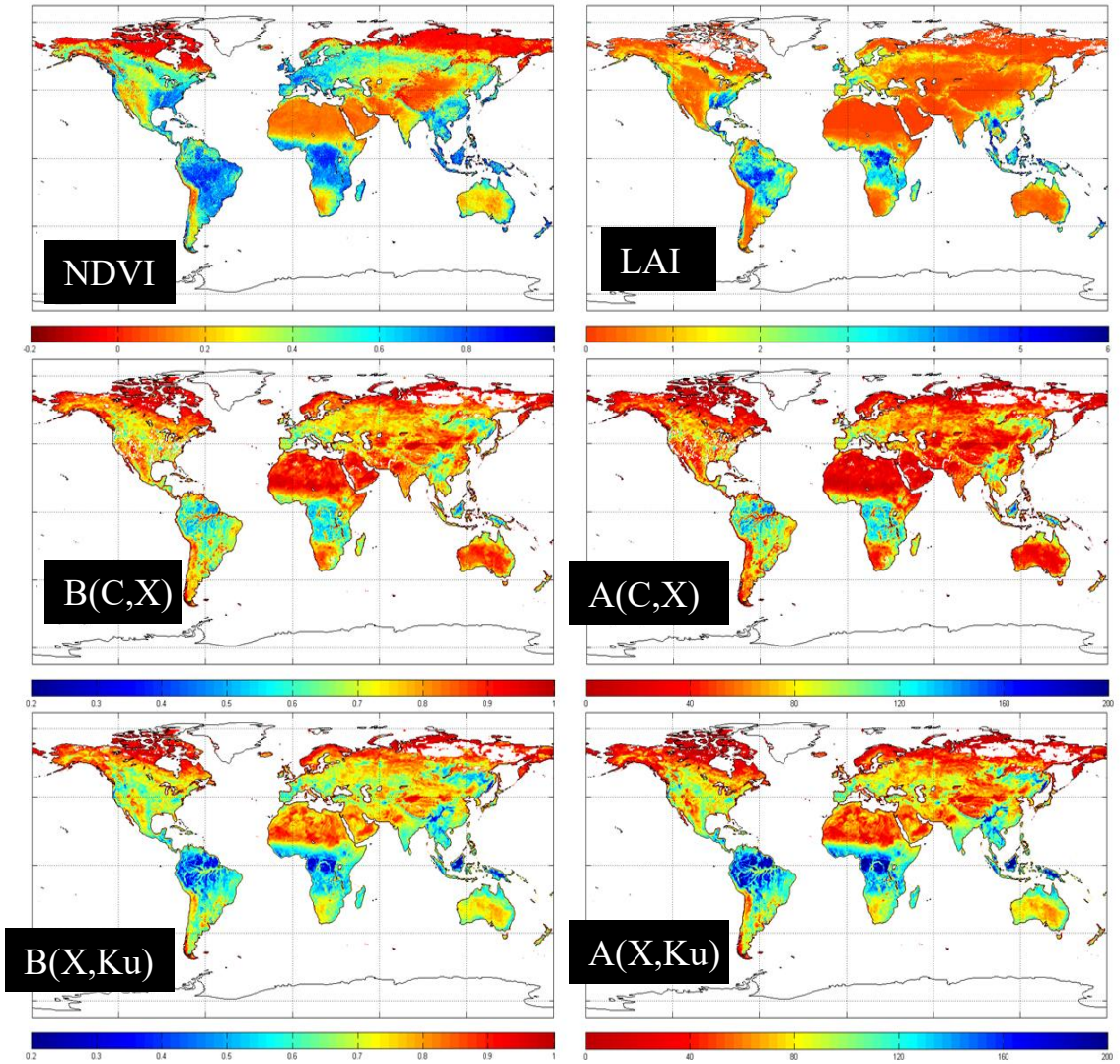

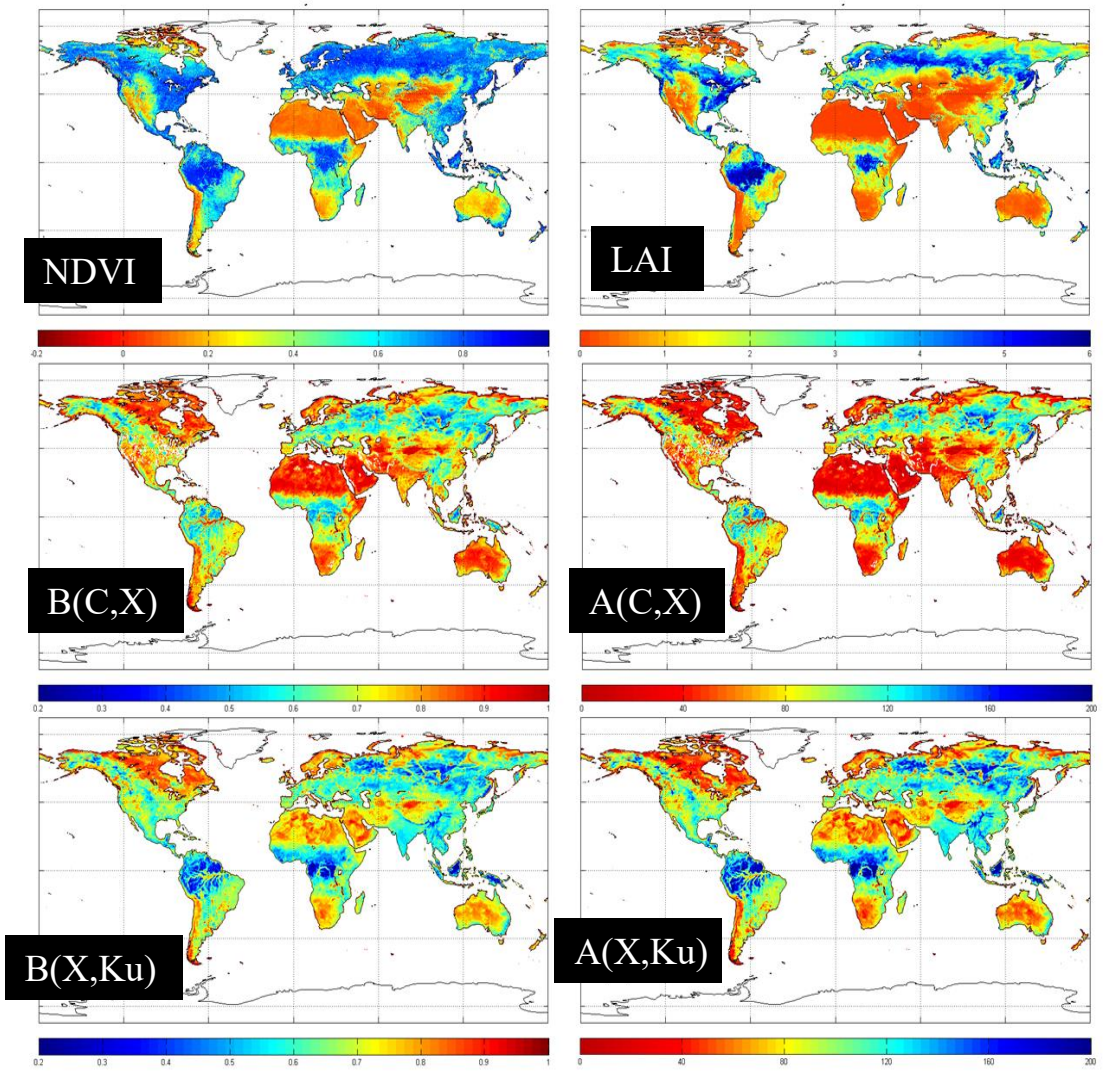

Examples of Correlations between MVIs and NDVIs

Correlations of the shrub land in Tibet

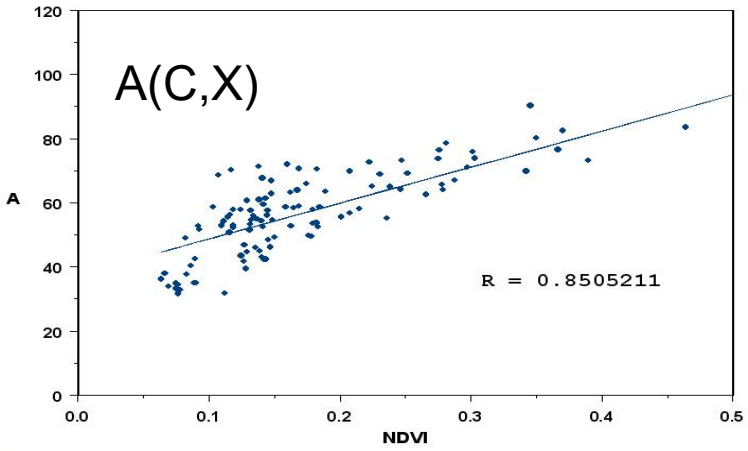

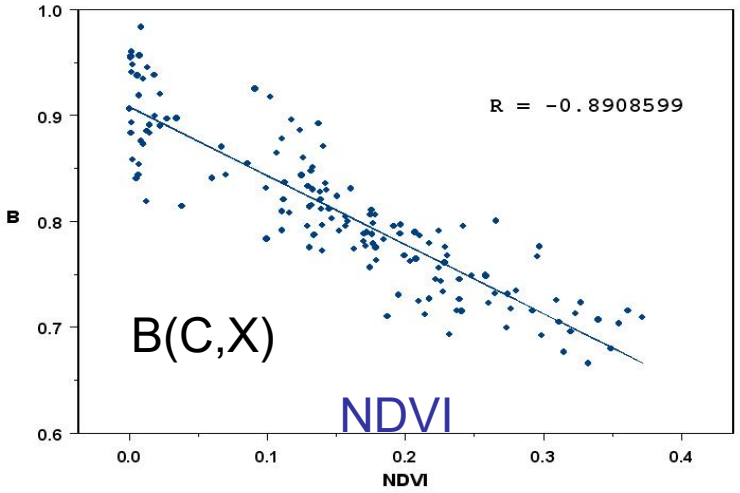

Correlations of the grass land in Mongolia

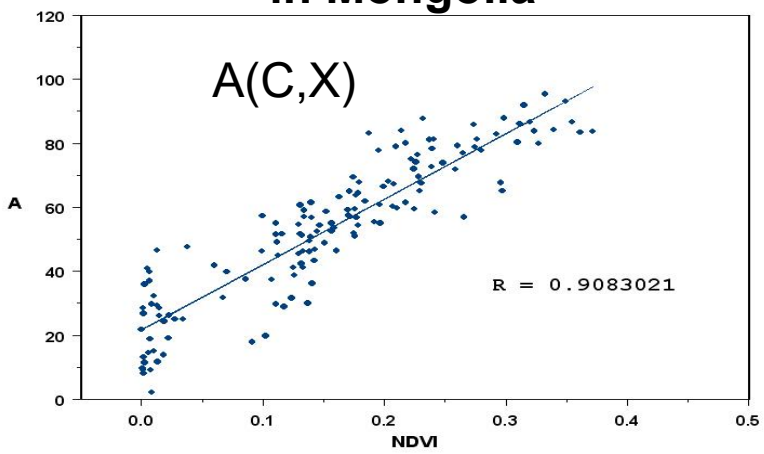

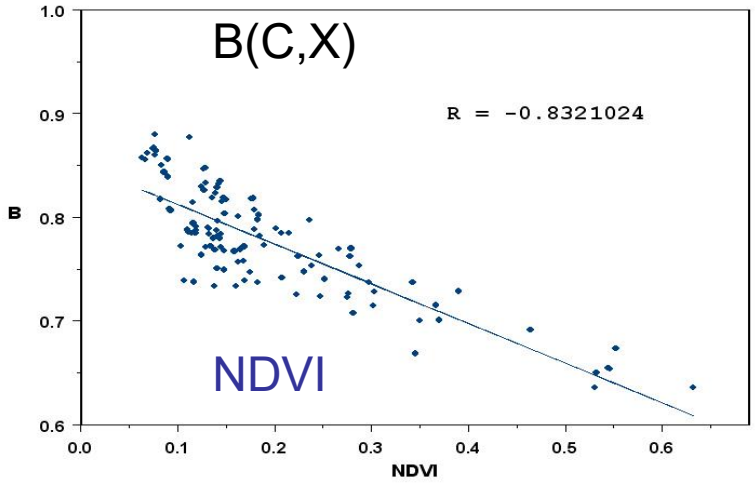

Global Statistics of Correlations

Land Covers	B(C,X)	B(X,Ku)	Land Covers	B(C,X)	B(X,Ku)
Deciduous Needle leaf Forest	0.837	-0.772	Grass land	-0.698	-0.696
Evergreen Needle leaf Forest	-0.652	-0.510	Shrub land	-0.553	-0.367
Savannas	-0.582	-0.433	Crop land	-0.508	-0.427
Deciduous Broad leaf Forest	-0.122	-0.538	Mixed Forest	-0.473	-0.441
Evergreen Broad leaf Forest	0.031	0.080	Bare Ground	-0.056	-0.024

NDIV vs. MVIs of Global Forests Samples

Correlation

Left column: NDVI vs. low frequency pair B parameters **-> For a given NDVI value, there are large MVIs variations;**

Right column: High frequency vs. low frequency pair B parameters -> **Different frequency pairs provide also significant different vegetation information;**

Indication: **MVIs Provide significant new vegetation information, especially sensitive to woody part of vegetation**

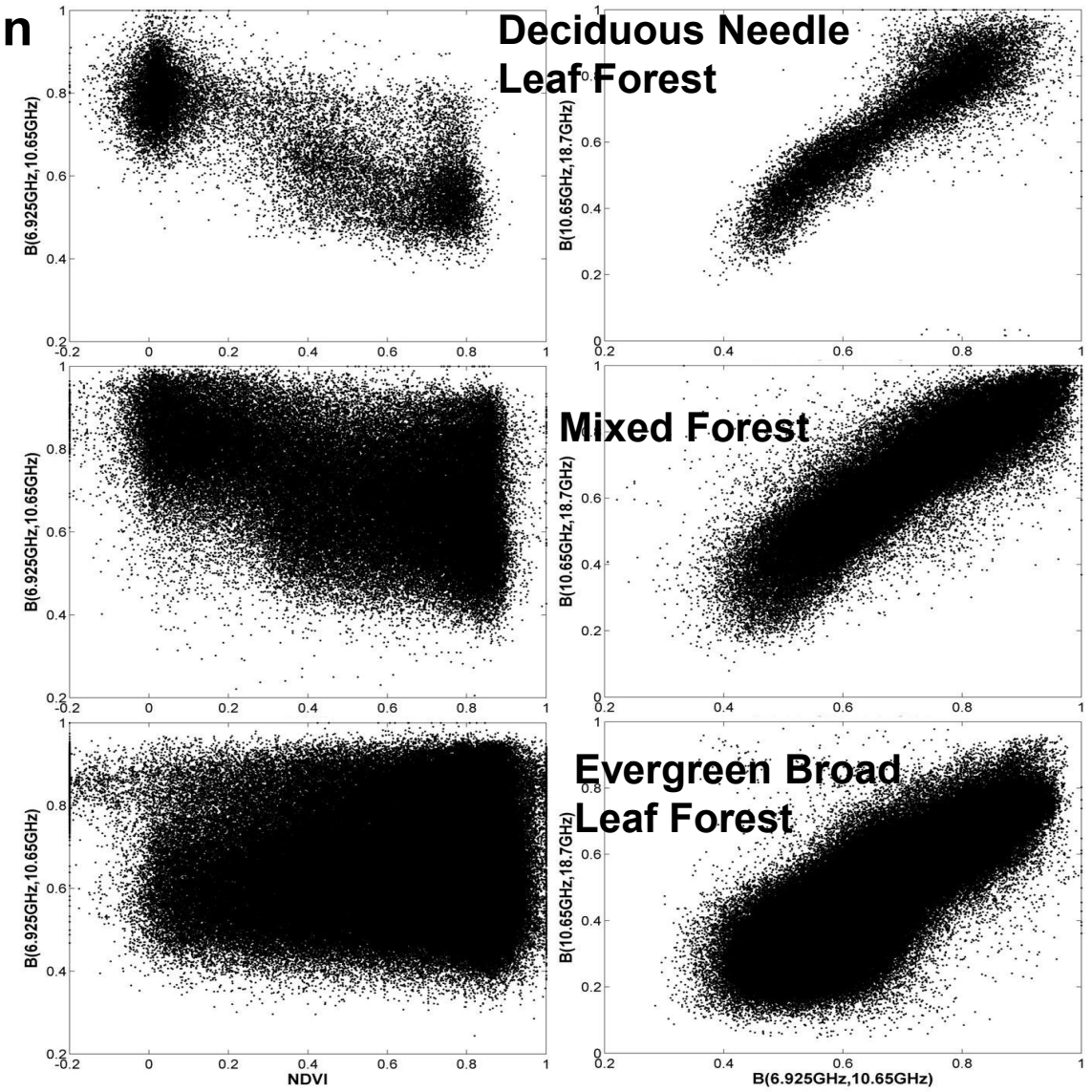

Summary on AMSR-E's MVIs

Comparison with NDVI and LAI measurements

- A similar global patterns in difference seasons;
- Provide vegetation phenology (seasonal variation) information;
- Good correlations in some land cover types, especially Grass and deciduous Needle Leaf Forest;
- Provide woody part vegetation information.

Developed microwave vegetation indices provide the potential of complementary dataset for global vegetation monitoring and applications.

This technique can be also applied to other passive microwave satellites like FY, AMSR-2,WINSAT, TMI/TRMM, and SSMR.

SMOS - Soil Moisture and Ocean Salinity

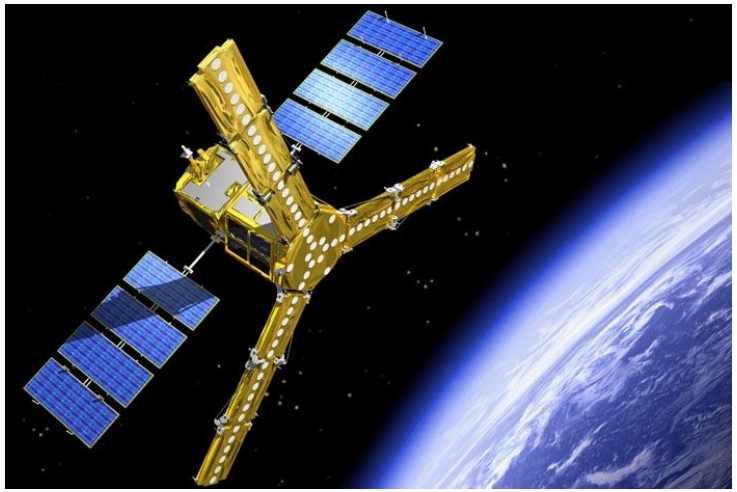

- ✓ Launched in November, 2009
- ✓ L-band (1.41 GHz) microwave radiometry by aperture synthesis
- ✓ Average spatial resolution of 43 km
- ✓ Repetition of 3 days
- ✓ 6am ascending, 6pm descending
- ✓ Y-shaped antenna with 3 arms (8 m) and a central hub

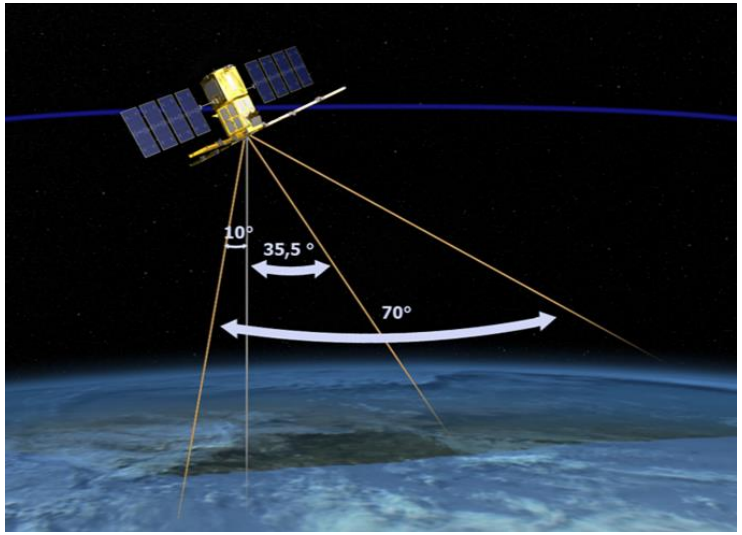

- ✓ Images acquired in a single snapshot for every 1.2 seconds
- ✓ Dual polarization and full polarization mode
- ✓ Field of view is about 70 degrees (-10~60)
- ✓ Ground footprint (snapshot) of about 1,000 km × 1,500 km

Angular Feature of Bare Soil Emission

AIEM simulations

Parameter	Min	Max	Interval	Unit
Incidence Angle	30	55	5	degree
Soil Moisture	2	44	2	%
rms	0.25	3.5	0.25	cm
Correlation Length	2.5	30	2.5	cm
Correlation Function	Gaussian ,1.5-Power and Exponential			

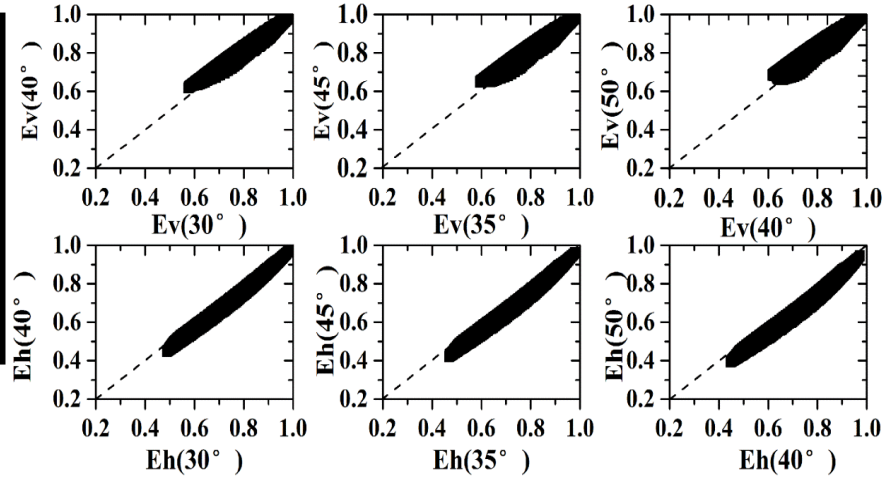

For H polarization:

(θ_1,θ_2)	a	b	R^2	RMSE
(30°,40°)	-0.0514	1.0208	0.9958	0.0082
(40°,50°)	-0.0632	1.0069	0.9925	0.011
(35°,45°)	-0.0577	1.0163	0.9944	0.0096

$$\varepsilon_p^s(\theta_2) = a_p(\theta_1,\theta_2) + b_p(\theta_1,\theta_2)\cdot\varepsilon_p^s(\theta_1)$$

Two reasons for only using H-polarized bright temperature to retrieve VOD:

(1) A stronger correlation was found between the bare soil emissivities at two incidence angles with 10° difference at H polarization ;

(2) vegetation has much stronger polarization dependence than that at higher frequencies.

H-polarized Multi-angular MVIs

$$TB_p(\theta)=[(1-\omega_p)\cdot(1-L_p(\theta))\cdot(1+L_p(\theta))]\cdot T_C+[L_p(\theta)\cdot T_s-(1-\omega_p)\cdot(1-L_p(\theta))\cdot L_p(\theta)\cdot T_C]\cdot\varepsilon_p^s(\theta)$$

$$TB_h(\theta)=V_{eh}(\theta)+V_{atth}(\theta)\cdot\varepsilon_h^s$$

$$\varepsilon_h^s(\theta_2)=a_h(\theta_1,\theta_2)+b_h(\theta_1,\theta_2)\cdot\varepsilon_h^s(\theta_1)$$

With two incidence angles' soil emission relation:

$$\frac{TB_h(\theta_2)-V_{eh}(\theta_2)}{V_{atth}(\theta_2)}=a_h(\theta_1,\theta_2)+b_h(\theta_1,\theta_2)\cdot\frac{TB_h(\theta_1)-V_{eh}(\theta_1)}{V_{atth}(\theta_1)}$$

$$TB_h(\theta_2)=a_h(\theta_1,\theta_2)\cdot V_{atth}(\theta_2)+V_{eh}(\theta_2)-b_h(\theta_1,\theta_2)\cdot\frac{V_{atth}(\theta_2)}{V_{atth}(\theta_1)}\cdot V_{eh}(\theta_1)+b_h(\theta_1,\theta_2)\cdot\frac{V_{atth}(\theta_2)}{V_{atth}(\theta_1)}\cdot TB_h(\theta_1)$$

Ah **Bh**

Ah and Bh are called H-polarized multi-angular MVIs which are functions of vegetation parameters and temperature.

Sensitivity of H-polarized multi-angular MVIs to vegetation parameters

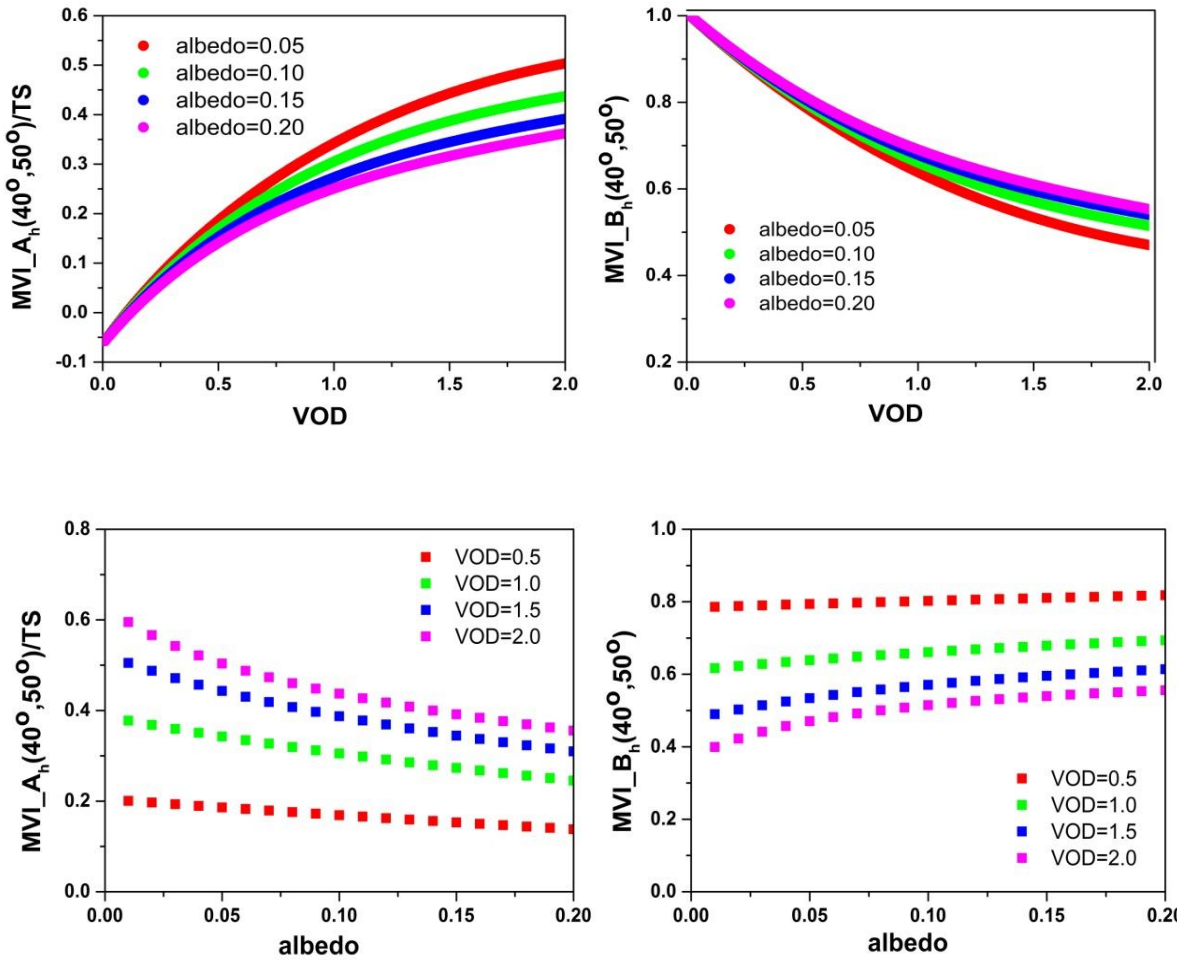

- MVIs are Highly sensitive to VOD;
- Lower sensitivity to vegetation single scattering albedo;
- Retrieving VOD is more effective.

Validation with Experimental Data

- With reliable ground-based measurements of soil moisture and temperature from the Litter Washita network, the indirectly measured VOD can be calculated using the H-polarized brightness temperature based on the tau-omega radiation transfer model with default value of 0.05 and 0.10 for vegetation single scattering albedo and roughness parameter h, respectively.

- These indirectly measured VOD are compared with our retrieved VOD from SMOS multi-angular brightness temperature data.

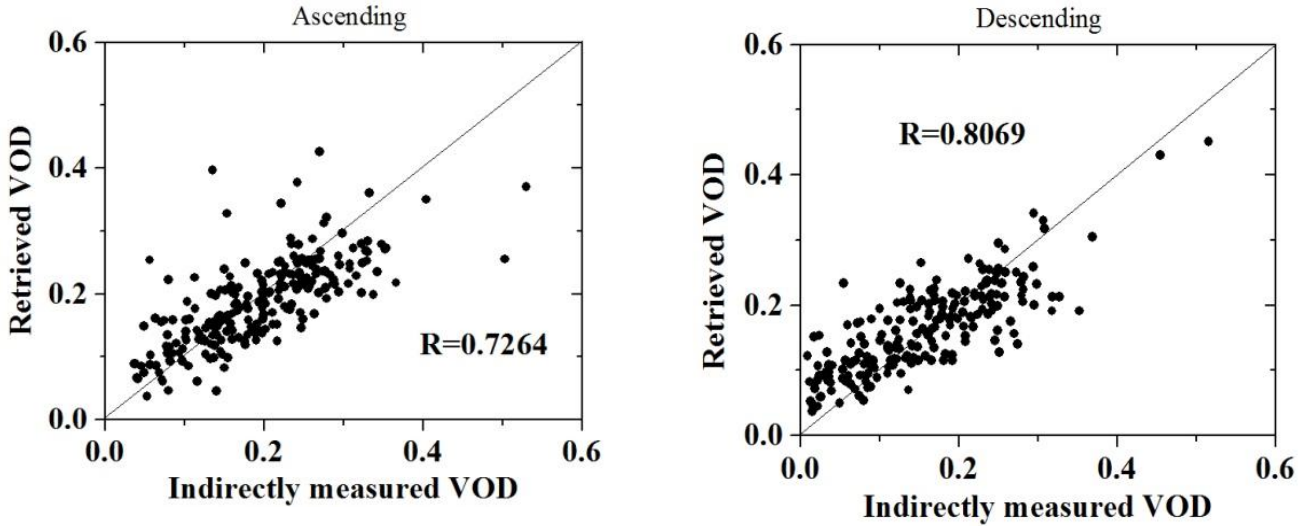

This retrieval method is feasible in SMOS's view

Vegetation Seasonal Change

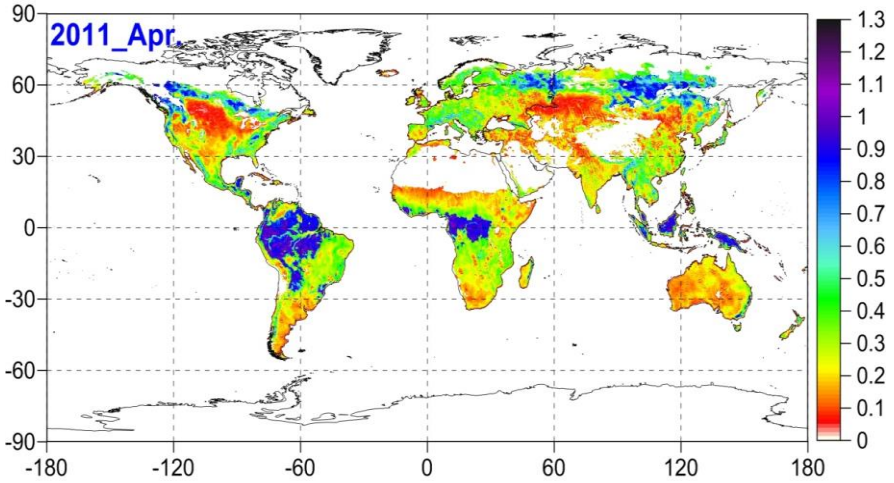

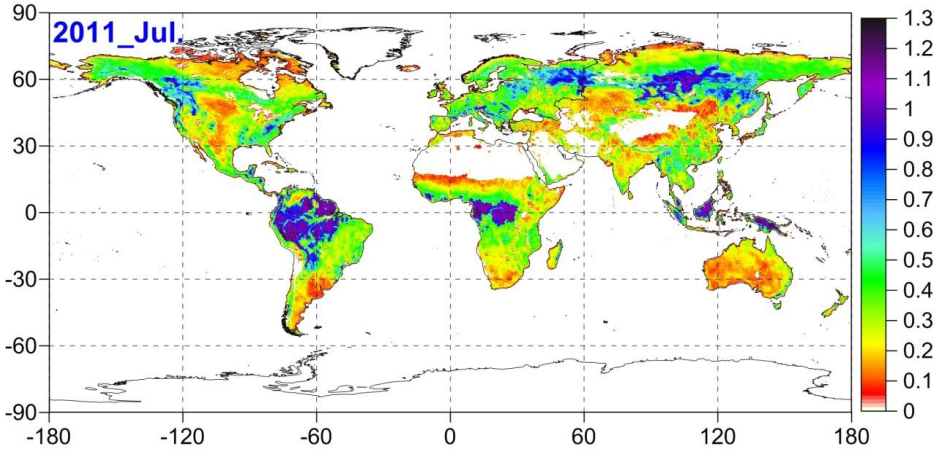

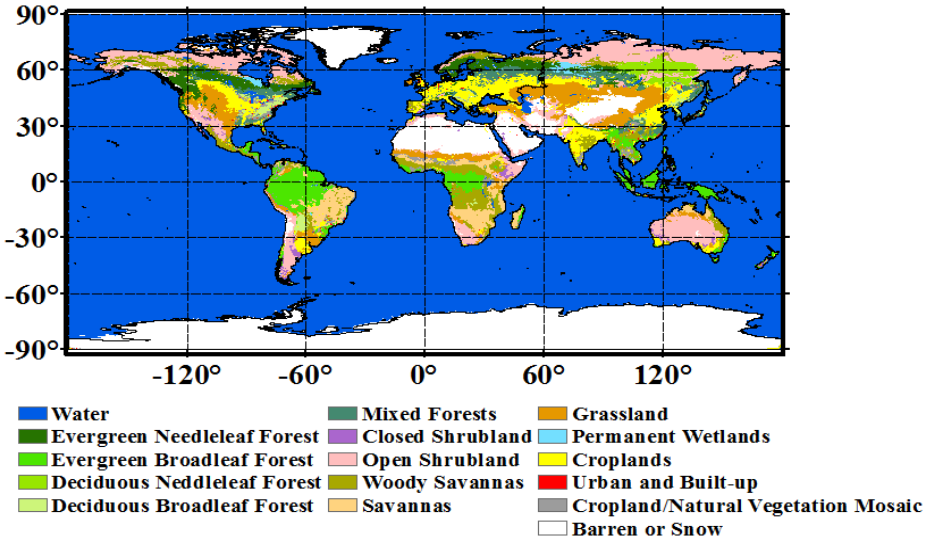

- Bare soil, frozen ground, snow and ice are flagged
- Spatial distribution is generally consistent with global land cover types
- Reasonable seasonal change

Comparison With Biomass

Aboveground biomass（Saatchi et al., 2011）

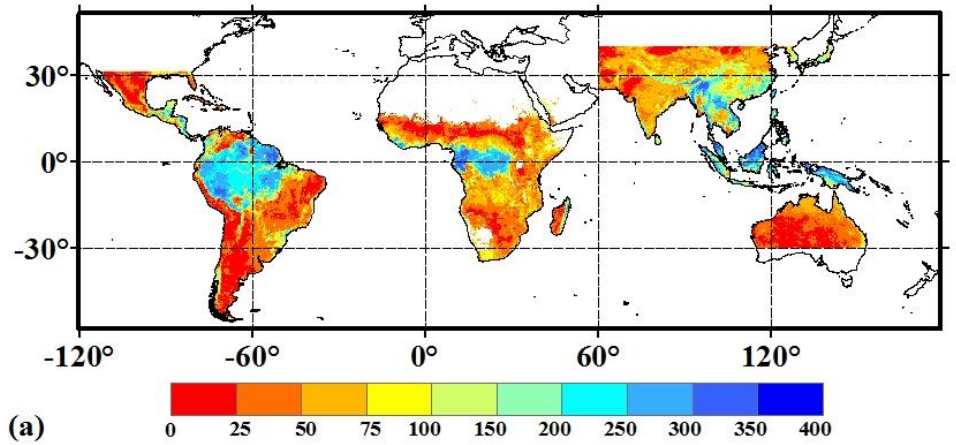

Retrieved VOD:

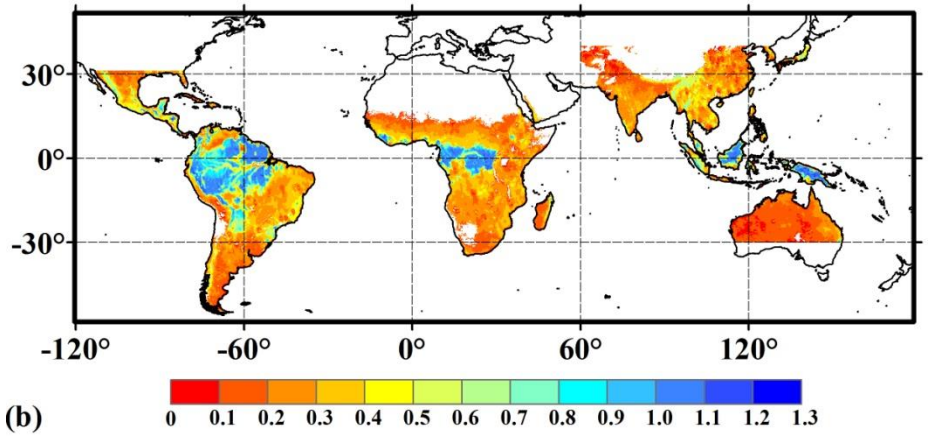

MODIS-NDVI

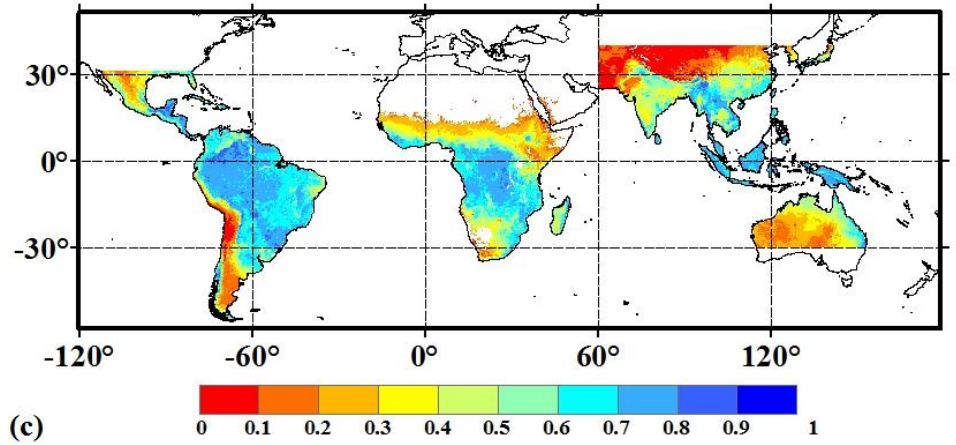

- The spatial distribution of the Above Ground Biomass (AGB) and retrieved VOD are consistent, and generally shows high values for forests and low values for short vegetation regions
- Differences exist between AGB and NDVI, which presents larger area of greenness

Summary on SMOS Applications

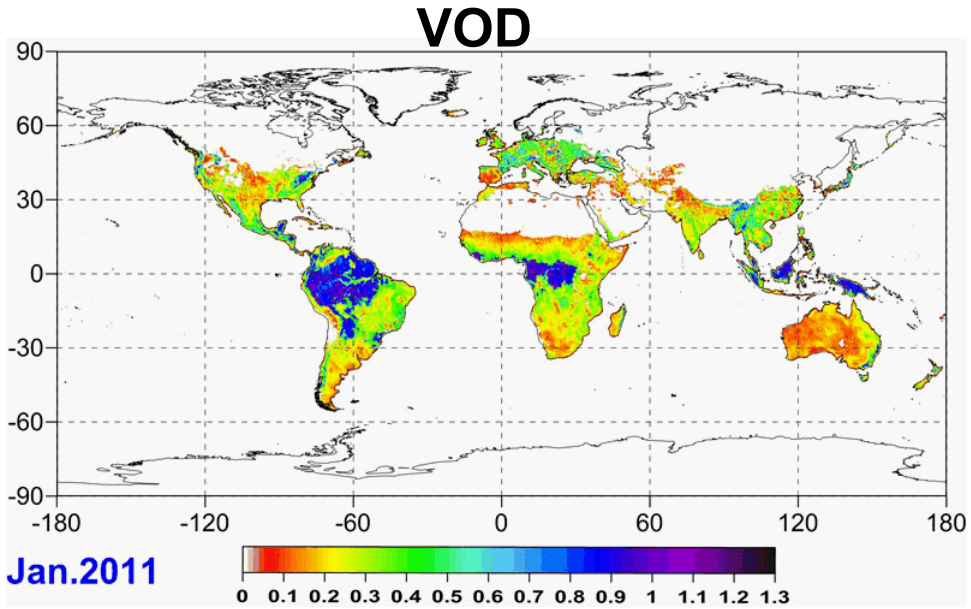

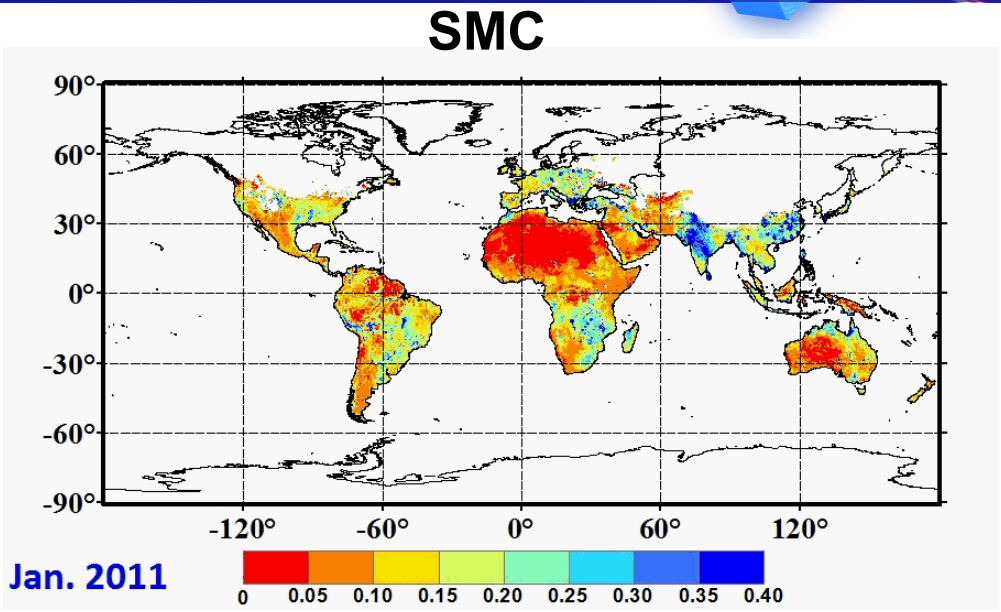

- **Based on the microwave vegetation index derived from multi-incidence angle measurements, we developed a simple algorithm for retrieving optical thickness and soil moisture**
- **VOD is dominated by vegetation water contents, structure, and biomass**
- **Higher order scattering model should be used for both MVIs and optical thickness estimation.**


FENGYUN Satellite User Conference
Qingdao China · 2025
AOMSUC-15 2025 FYSUC
THE 15TH ASIA-OCEANIA METEOROLOGICAL SATELLITE USERS' CONFERENCE (AOMSUC-15)
2025 FENGYUN SATELLITE USER CONFERENCE (2025 FYSUC)
Thank you for attention!
shijiancheng@nssc.ac.cn